Plasmon-enhanced photoresponse of deep-subwavelength GaAs NW photodetector*

LI Bang (李邦)[1,2,3]**,**TANG Yanni** (唐燕妮)[4], **YAN Xin** (颜鑫)[4], **ZHANG Xia** (张霞)[4], **and LIU Yongge** (刘永革)[1,2,3]

1. School of Computer & Information Engineering, Anyang Normal University, Anyang 455000, China

2. Key Laboratory of Oracle Bone Inscriptions Information Processing, Ministry of Education of China, Anyang 455000, China

3. Henan Key Laboratory of Oracle Bone Inscriptions Information Processing, Anyang 455000, China

4. State Key Laboratory of Information Photonics and Optical Communications, Beijing University of Posts and Telecommunications, Beijing 100876, China

(Received 16 July 2020; Revised 4 October 2020)

According to optical diffraction limit, the photoresponsity of nanowire (NW)-based photodetector exponentially decreases when its NW diameter reduces to the range of deep subwavelength. In this paper, we demonstrate a photoresponse-enhanced method of the deep-subwavelength GaAs NW photodetector by using a plasmon-driven dipole antenna. Considering that the enhancement is extremely influenced by the shape and size of antenna, the structure of antenna is optimized by finite difference time domain (FDTD) solutions. The optimal structure of antenna optimizes the responsivity-enhanced factors to 1123.3 and 224.7 in NW photodetectors with NW diameters of 20 nm and 60 nm, respectively. This photoresponse-enhanced method is promising for easy-integration high-performance nanoscale photodetectors.

Document code: A **Article ID:** 1673-1905(2021)07-0385-5

DOI https://doi.org/10.1007/s11801-021-0120-8

Semiconducting nanowires (NWs) excite great research interest due to the possibility of their application in many nanoelectronics and photonics devices[1-3]. Compared with thin film materials used in optoelectronics[4], the NWs present unique properties , such as high NW length-to-diameter ratios, high surface-to-volume ratios, high crystal quality, and nanometric foot-prints, allowing them to show quantum effects[1], surface optical phonons[2], ultra-high photo-gains[3], as well as, higher signal-to-noise ratios[5], higher sensing surface[6], and higher mechanical properties[7]. In the case of photodetectors, most researches focus on the metal-semiconductor-metal (MSM) architecture with either ohmic or Schottky contacts[8-10]. Such devices present high gain but they are strongly sublinear and their time response is generally in the range of millisecond. When the target is a quantitative measurement of the incident radiation, PN photodiodes are generally preferred over metal-semiconductor-metal architectures because of their lower dark current and the linearity of their response[11].

GaAs NWs show particular promise in high-speed photodetectors owing to their high absorption coefficient and direct bandgap[8-10]. The growth of GaAs with axial PN junction has been widely reported[12,13]. However, the investigation of photodetector with deep-subwavelength GaAs NWs still remains a difficult task, which is mainly caused by the optical diffraction limit in the medium. The optical diffraction limit directly results in intrinsically poor optical confinement within the NW[14,15]. In research of photodetector, optical confinement is an essential factor which is closely related to the photoresponse[16]. One solution of this problem is to confine and trap light into a deep-subwavelength NW by nonstructural metallic particles[17-22]. In this way, photoresponse is enhanced by light-matter coupling owing to the excitation of collective electron oscillations, known as localized surface plasmon resonance (LSPR)[23]. In addition to metallic particles, nanostructural metallic antennas are also devoted to enhance the process of light-matter coupling into NW[24-26]. However, in the investigation of reported plasmon-driven photodetectors, the structure of antennas is not consistent. To our best knowledge, the

* This work has been supported by the National Natural Science Foundation of China (Nos.61774021, 61806007 and 61911530133), the Fund of State Key Laboratory of Information Photonics and Optical Communications (Beijing University of Posts and Telecommunications), China (No.IPOC2019ZT07), the Fundamental Research Funds for the Central Universities (No.2018XKJC05), the Project of Key Science and Technology in Henan Province (No.202102310562), the Fund of Key Laboratory of Oracle Bone Inscriptions Information Processing, Ministry of Education of China (No.OIP2019M006), the Research Foundation of Anyang Normal University (No.AYNUKPY-2019-04), and the Anyang Scientific and Technological Project (No.2021C01X012).

** E-mail: 01782@aynu.edu.cn

plasmon-driven light enhancement effect of the antenna structure hasn't been systematically investigated in the deep-subwavelength NW-based photodetector. Thus, realizing the high-performance photodetector with a deep-subwavelength structure is of great significance in future optical communication.

In this paper, we investigate the plasmon-driven light enhancement effect of plasmatic antennas in a deep-subwavelength GaAs NW photodiode. In particular, we use Au dipole antenna to concentrate light from a large optical area into the PN junction of GaAs NW. Compared with bare NW photodetector, the photodetector with dipole antenna exhibits a higher responsivity due to LSPR. Moreover, considering that the optical properties of plasmonic antenna are largely depended on its size and shape, the maximum of photoresponsivity can be achieved by modifying the antenna structure. The light confinement of plasmonic antenna is calculated by the finite difference time domain (FDTD) method in which Maxwell's time dependent curl equations are solved by a three-dimensional grid, while the optical generation and responsivity of photodetectors are evaluated through another software of Lumerical-DEVICE.

A schematic of the proposed structure is illustrated in Fig.1. In the FDTD calculations, our device is consisted of a contacted axial PN junction GaAs NW and an Au dipole antenna. The plane wave is excited along the z axis and the light polarization is parallel to the dipole antenna (y polarized). The Au open-sleeve dipole antenna has a dipole oriented along the y direction on both sides of the junction area of axial PN NW, which can be located by cathodoluminescence measurements in the DEVICE simulation[12]. Perfectly matched layer (PML) boundary conditions are used to absorb outgoing waves from the computational domain, ensuring a perfect absorption of electromagnetic radiation at the simulation boundaries. Besides, a low index, non-absorbing substrate is necessary to maximize mode confinement to the NW (for larger modal gain) and minimize optical losses, both of which contribute to maximizing the detection sensitivity of the NW detector.

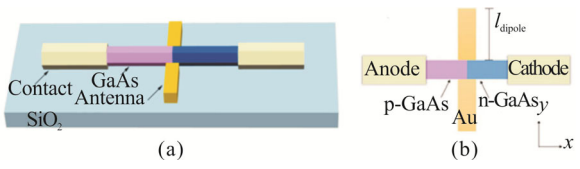

Fig.1 The schematic of the device: (a) Illustration of a contacted axial PN junction GaAs NW with a dipole antenna on its both sides; (b) Top view of the open-sleeve dipole antenna consisting of a dipole antenna

In modeling of photodetector, the length of the regular hexagon GaAs NW is 2 μm, the thickness of the dipole antenna is 50 nm. The substrate is SiO_2 (with a refractive index, n=1.45). The wavelength of incident light is 850 nm, which is the first low loss window of optical communication. The length of antenna is calculated as 116.5 nm by the equation $L=\lambda/(2n)$, where n is the refractive index of GaAs, and λ is the resonance wavelength[25,27]. Moreover, the distance between the cathode and anode electrode is set as the barrier width of PN junction (190 nm), which is calculated by

$$W \approx W_{\mathrm{n}} = \sqrt{V_{\mathrm{D}}\left(\frac{2\varepsilon_{\mathrm{r}}\varepsilon_0}{q}\left(\frac{N_{\mathrm{A}}+N_{\mathrm{D}}}{N_{\mathrm{A}}N_{\mathrm{D}}}\right)\right)}\ , \tag{1}$$

where ε_{r} is relative permittivity for GaAs, ε_0 is the permittivity of free space, N_{A} is acceptor concentration, N_{D} is the donor concentration, V_{D} is the built-in potential difference of PN junction, which is calculated as

$$V_{\mathrm{D}} = \frac{KT}{q}\ln\frac{N_{\mathrm{A}}N_{\mathrm{D}}}{n_{\mathrm{i}}^2}\ , \tag{2}$$

where n_{i} is the intrinsic carrier concentration.

Simulated by DEVICE, the 3D optical generation profiles are incorporated into the finite-element mesh of the NWs in the electrical tool to fabricate the electrical modeling partial. The simulated photoresponse of device are calculated in reverse bias. The doping-dependent mobility (GaAs only), bandgap narrowing, radiative, Auger and Shockley-Reed-Hall (SRH) recombination are all taken into consideration. The material parameters critical for device simulations are obtained from the Povinelli model[28].

The spectral dependence of optical absorption in NW can be strongly influenced by its diameter[29,30]. In the FDTD simulation, the light absorption is mainly affected by the effective index of leaky modes. As the optical power amplitude shown in Fig.2(a), when the diameter of the GaAs NW is less than 100 nm, the optical modes are not confined in the NW and the optical absorption of the NW exponentially decreases with its diameter, which is consistent with the resonant optical phenomena[31]. Consequently, the deep subwavelength NW-based photodetectors exhibit an unsatisfying performance as shown in Fig.2(a). The photoresponse decreases from 0.132 A/W to 0.006 A/W when the NW diameter varies from 90 nm to 20 nm. As mentioned above, the device performance is sensitive to its scale and the weak optical absorption of NW becomes a stumbling block in reducing the device scale. In the pursuit of high-performance photodetector, the method of confining light into NW should be proposed to improve the photoresponse.

The confinement of strong optical near fields in a subwavelength volume by the resonant antenna has been discussed in previous reports[32,33]. By coupling plasmon excitation of Au antenna into NW, the hybrid system formed by a GaAs NW with a PN junction and an Au dipole antenna causes an additional possibility of optical absorption, especially in the local enhancement of absorption with deep subwavelength diameter NWs. According to the collective electron current oscillations via Ampere's law, the high electromagnetic fields at a metal/air interface decays rapidly into the metal and dielectric[19]. The power distribution in the NW is affected by the interaction between the NW modes and antenna plasmonic

modes. As depicted in Fig.3(a), the comparison of power amplitude and optical generation between the NW with (right) and without (left) the dipole antenna perspicuously exhibits the enhancement of optical absorption in the antenna-decorated NW. The incident light is observed to be coupled from the Au dipole antenna into GaAs NW, leading to a remarkable portion of optical absorption in the NW of varies diameters, such as 30 nm, 60 nm, and 90 nm shown in Fig.3(b). Consequently, the photoresponse is enhanced due to the photogenerated electron-hole pairs excited by the trapped light. In order to investigate the photoelectric conversion characteristic, the structure and optical absorption data are imported into DEVICE for further calculation. As illustrated in Fig.3(c), a significant enhancement of photoresponsivity is observed while the NWs are decorated by dipole antennas. The calculated photoresponsivities of antenna-enhanced NW-based photodetector ranges from 4.14 A/W to 17.4 A/W with antenna-driven enhancement factors of 13 to 576. As mentioned above, the photoresponsivities of bare NW-based photodetector are positively correlated with their NW diameters. However, the trend of enhanced photoresponsivities is not a monotone transformation, which can be attributed to the dipole antenna size of the device with varied NW diameters. The enhancement effect of same antenna structure shows distinct differences on diverse photodetector structures, for the reason that LSPR of antenna is sensitive to the size of device. Therefore, the detection performance could be improved by optimizing the antenna structure.

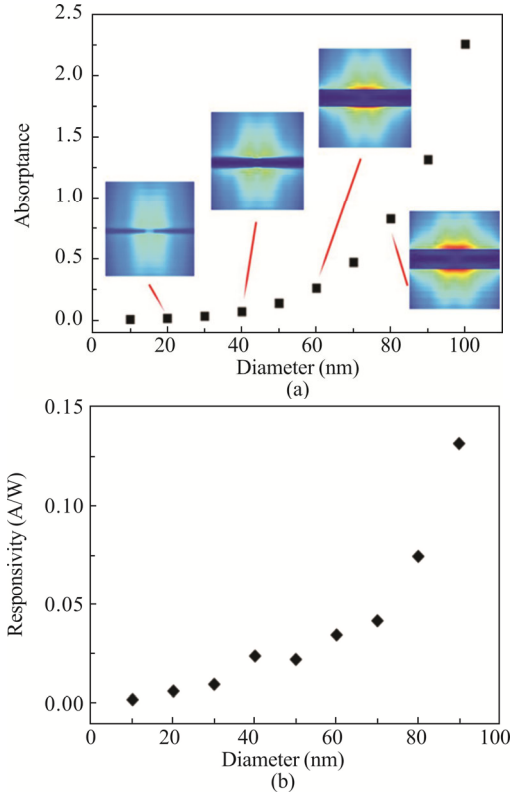

Fig.2 (a) FDTD-simulations of absorption efficiency (AE), which plotted as a function of diameter of NW; (b) The DEVICE-calculated photoresponsivity of the GaAs NW photodetector with λ=850 nm changed with NW diameter

To our knowledge, the structure of antenna in plasmon-driven photodetector has not been systematically studied yet. The performance of plasmon-driven photodetector could be improved by adjusting the size and shape of its antenna due to its stricture sensitivity[26]. However, in the investigation of plasmon-driven photodetectors, the shapes of antennas are not consistent[24,25]. In the pursuit of high photoresponsivity, FDTD simulations are carried out to obtain the optimum shape and size of antenna as depicted in Figs.4 and 5, respectively. The shape of antenna is designed to be two tip- to-tip triangles with varied tip angles changed from 0° to 180°. It should be point out that the antenna becomes "linear" when the angle is 0° and becomes "circular" when the angle is 180°. As the power distribution shown in Fig.4(a), the optical power in the NW increases with the declined tip angle of antennas. That is, the field intensity in NW is observed to be higher with a sharper antenna tip, which can be attributed to that the charges on the antenna surface are confined to a smaller area due to the decreasing current distribution[27].

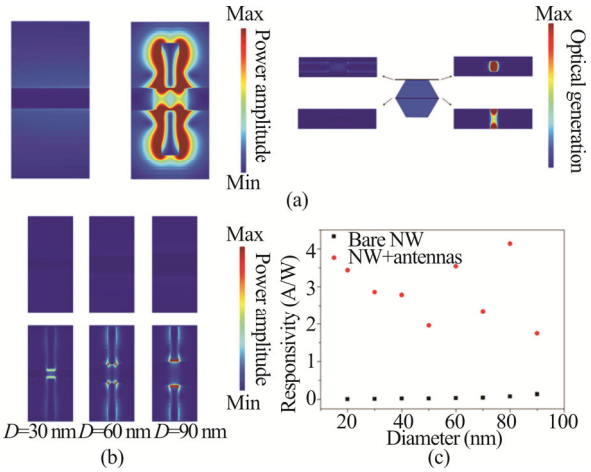

Fig.3 (a) FDTD-simulated distribution of optical power intensity and optical generation of GaAs NW decorated with or without antenna; (b) FDTD-simulated distribution of optical power intensity in GaAs NW with diameters of 30 nm, 60 nm and 90 nm, respectively; (c) A plot of the responsivity of the detector for the competition between NW decorated with a dipole antenna and without antenna

Considering that the optical field confined into NW reflects the surface charge density, the photo-generated current in NW is supposed to be increased due to the enhanced surface charge density. Therefore, the photoresponsivities calculated by DEVICE also increase with the enhanced surface charge density as shown in Fig.4(b). The trend of responsivities changed with tip angles is consistent with the power distribution ampli-

tude of NW, as shown in Fig.4(a). The highest enhancement of the photoresponsivity is obtained when the tip angle is 0°, suggesting that the "linear" shape is the optimum shape of antenna for the photodetector.

Furthermore, as the "linear" shape antenna can be considered as a rectangle, the optimum size of antenna is entirely decided by the length and width of the rectangle.

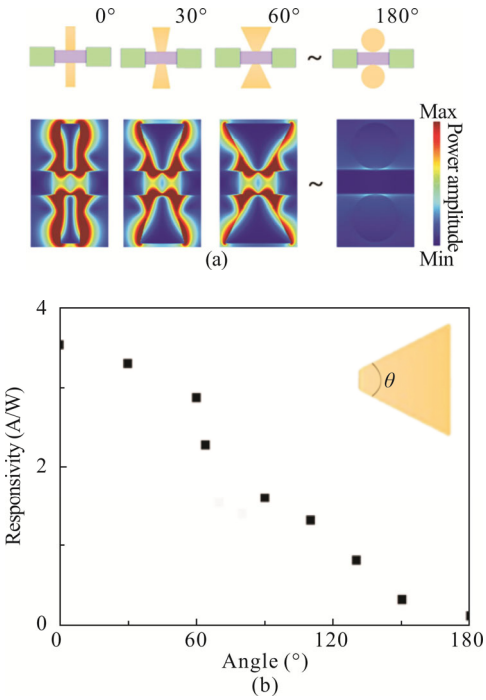

Fig.4 (a) FDTD-simulated power intensity of the device versus tip-angle of triangular antenna, where the tip-angle of the antenna changes from 0° (linear antenna) to −180° (circular antenna); (b) The responsivity of the device changed with the tip-angle of the triangular antenna

As mentioned above, the length of antenna is related to the wavelength of incident light (a length of 116.5 nm related to the wavelength of 850 nm), while the diameter of antenna (the width of the rectangle) for maximized local field enhancement has not been addressed. Obviously, when the antenna width approaches zero, the nearly "nonexistent" antenna can hardly restrict electromagnetic fields. On the contrary, if the antenna is too wide, the optical field also can't be concentrated into NW for the reason that the antenna tip is no longer "sharp". In FDTD simulations, we focus on the optimum width of antenna based on the NW diameter of 20 nm and 60 nm. As shown in Fig.5(a), the responsivities do not monotonically change with the width of antenna and two peaks are observed in the photoresponsivities of both photodetectors, which is consistent with the distribution density of optical generation show in Fig.5(b). When NW diameter is 20 nm, the peaks are 6.74 A/W and 4.92 A/W at the antenna diameter of 30 nm and 65 nm respectively, while the photoresponsivity peaks of the 60 nm NW-diameter photodetectors are 4.48 A/W and 7.64 A/W at the antenna diameter of 25 nm and 50 nm, respectively. Compared with the photoresponsivity with a bare NW, the highest enhancement factor of the 20 nm NW-diameter photodetector is 1 123.3 with an antenna width of 30 nm, while the highest enhancement factor of the 60 nm NW-diameter photodetector is 224.7 with an antenna width of 50 nm. The optimum widths of antenna are inconformity between the two NW-diameters which can be attributed to the size sensitivity of plasmon-driven antenna. It should be point out that the width of the antenna in experiment should be limited by the lithography accuracy of electron beam lithography. Therefore, the theoretical maximum of photoresponse is hard to be achieved due to the experimental accuracy deviation. However, the average enhancement factor of photoresponsivity is still observed to be more than 100 near the width peak, suggesting that the fabrication of nanoantenna has experimental feasibility and the dipole antenna resonance plays an important role in the deep subwavelength GaAs photodetectors.

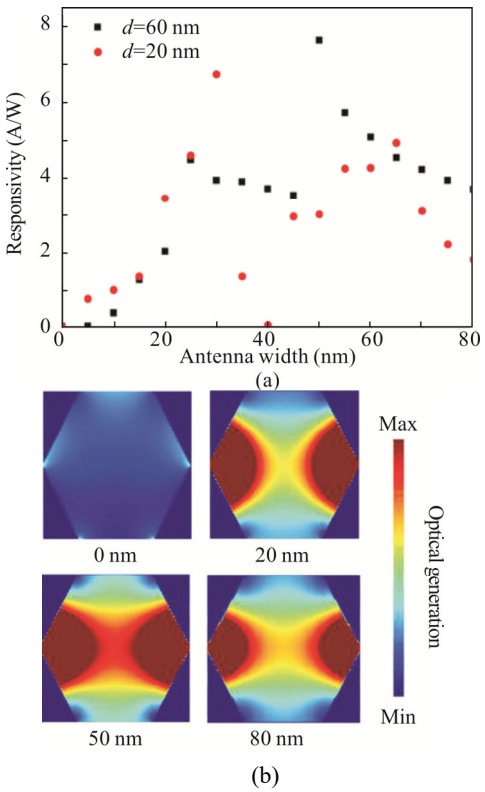

Fig.5 (a) A plot of the responsivity enhancement as a function of the width of the antenna; (b) The sectional optical generation distribution in the NW with the width of dipole antenna of 0 nm, 20 nm, 50 nm and 80 nm, respectively

In conclusion, we proposed a PN photodetector based on single GaAs NW decorated by a dipole antenna. A 3D employed FDTD method in optical simulation and optoelectronic simulation are used to evaluate the performance of the photodetector with/without dipole antenna on both sides of NW. Decorated by a dipole antenna, the

photodetector exhibits an enhanced responsivity, which is further improved by optimizing the size and shape of antenna. The optimum sizes of the "linear" shape are proved to be a length of 116.5 nm and a width of 30 nm and 50 nm for the photodetector with a NW-diameter of 20 and 60, respectively. The relative photoresponsivities enhancement factor are calculated to be 1 123.3 and 224.7 correspondingly. The method of enhancing light-matter coupling by a dipole antenna provides an efficient way to dramatically improve the responsivity of deep subwavelength GaAs photodetectors.

References

[1] Kim W, Dubrovskii V G, Vukajlovic-Plestina J, Tütüncüoglu G, Francaviglia L, Güniat L, Potts H, Friedl M, Leran J and Fontcuberta i Morral A, Nano Lett. **18**, 49 (2018).

[2] García Núñez C, Braña A F, Pau J L, Ghita D, García B J, Shen G, Wilbert D S, Kim S M and Kung P, J. Appl. Phys. **115**, 034307 (2014).

[3] García Núñez C, García Marín A, Nanterne P, Piqueras J, Kung P and Pau J L, Nanotech. **24**, 415702 (2013).

[4] Wang G, Zhang Y, You C, Liu B, Yang Y, Li H, Cui A, Liu D and Yan H, Infrared Phys. Tech. **88**, 149 (2018).

[5] Rajan N K, David A R and Mark A R, Appl. Phys. Lett. **98**, 264107 (2011).

[6] Xie P, Xiong Q, Fang Y, Qing Q and Lieber C M, Nat. Nanotechnol. **7**, 119 (2012).

[7] Núñez C G, Liu F, Navaraj W T, Christou A, Shakthivel D and Dahiya R, Microsyst. Nanoeng **4**, 1 (2018).

[8] Ali H , Zhang Y , Tang J , Peng K, Sun S S, Sun Y, Song F, Falak A, Wu S, Qian C, Wang M, Zuo Z and Jin K , Small **14**, 01704429 (2018).

[9] Luo Y, Yan X, Zhang J, Li B, Wu Y, Lu Q, Jin C, Zhang X and Ren X, Nanoscale **10**, 9212 (2018).

[10] Cammi D , Rodiek B , Zimmermann K , Kuck S and Voss T, J. Mater. Res. **32**, 2464 (2017).

[11] Núñez C G, Braña A F, López N, Pau J L and García B J, Nanotech. **31**, 225604 (2020).

[12] Nägelein A, Timm C, Schwarzburg K, Steidl M, Kleinschmidt P and Hannappel T, Sol. Energ. Mat. Sol. C **197**, 13 (2019).

[13] Barrigón E, Hultin O, Lindgren D, Yadegari F, Magnusson M H, Samuelson L, Johansson L I M and Björk M T, Nano Lett. **18**, 2 (2018).

[14] Novotny L, Hecht B and Keller O, Phys. Today **60**, 62, (2006).

[15] Hauswald C, Giuntoni I, Flissikowski T, Gotschke T, Calarco R, Grahn H T, Geelhaar L and Brandt O, ACS Photo. **4**, 52 (2016).

[16] Soci C, Zhang A, Bao X Y, Kim H, Lo Y and Wang D, J. Nanosci. and Nanotech. **10**, 1430 (2010).

[17] Chen R, Li D, Hu H, Zhao Y, Wang Y, Wong N, Wang S, Zhang Y, Hu J, Shen Z and Xiong Q, J. Phys. Chem. C, **116**, 4416 (2012).

[18] Colombo C, Krogstrup P, Nygård J, Brongersma M L and Fontcuberta i Morral A, New J. Phys. **13**, 123026 (2011).

[19] Hyun J K and Lauhon L J, Nano Lett. **11**, 2731 (2011).

[20] Zhang X, Liu Q, Liu B, Yang W, Li J, Niu P and Jiang X, J. Mater. Chem. C **5**, 4319 (2017).

[21] Knight M W, Grady N K, Bardhan R, Hao F, Nordlander P and Halas N J, Nano Lett. **7**, 2346 (2007).

[22] Jee S W, Zhou K, Kim D W and Lee J H, Nano Converg. **1**, 29 (2014).

[23] Polman A and Catchpole K R, Opt. Exp. **16**, 21793 (2008).

[24] Casadei A, Pecora E F, Trevino J, Forestiere C, Rüffer D, Russo-Averchi E, Matteini F, Tutuncuoglu G, Heiss M, Fontcuberta i Morral A and Dal Negro, Nano Lett. **14**, 2271 (2014).

[25] Tang L, Kocabas S E, Latif S, Okyay A K, Lygagnon D, Saraswat K C and Miller D A B, Nature Photo. **2**, 226 (2008).

[26] Hao E and Schatz G C., J. Chem. Phys. **120**, 357 (2004).

[27] Crozier K B, Sundaramurthy A, Kino G S and Quate C F, J. Appl. Phys. **94**, 4632 (2003).

[28] Huang N, Lin C and Povinelli M L, J. Appl. Phys. **112**, 001948 (2012).

[29] Cao L, White J S, Park J S, Schuller J A, Clemens B M and Brongersma M L, Nature Mater. **8**, 6432009 (2009).

[30] Seo K, Wober M, Steinvurzel P, Schonbrun E, Dan Y, Ellenbogen T and Crozier K, Nano Lett. **11**, 1851 (2011).

[31] Mie G., Ann. Phys-Berlin, **330**, 377 (2010).

[32] Mühlschlegel P, Martin O J F, Hecht B, Hecht B and Pohl D W, Science **308**, 1607 (2005).

[33] Yuan Z, Li X, Guo Y and Huang J, Optoelectronics Lett. **11**, 13 (2015).